MOMENTUM TRANSFER IN THE PERIODICALLY PERTURBED TURBULENT SEPARATED FLOW OVER THE BACKWARD-FACING STEP

Shuya Yoshioka, Shinnosuke Obi and Shigeaki Masuda
Department of Mechanical Engineering, Keio University,
3-14-1, Hiyoshi, Kouhoku-ku, Yokohama, 223-8522, Japan.

ABSTRACT

The effect of artificially imposed periodic perturbation on the momentum transfer across the turbulent separated shear layer was experimentally investigated. The backward-facing step flow was chosen for the test case, where the perturbation was introduced as a direct suction and injection at the step edge. The velocity field was measured by a particle imaging velocimetry (PIV), which enables the observation of the large-scale vortex motion widely distributed in the separated shear layer. The data were phase-averaged, synchronizing with the perturbation, thus enabling the observation of the evolution of vortex pattern. It was revealed that the large scale vortices were introduced into the shear layer by the periodic perturbation. Investigation on the turbulent quantities based on the Reynolds averaged Navier-Stokes equation clarified that the vortex motion enhances the momentum transfer across the shear layer and promotes the reattachment.

INTRODUCTION

The control of separated flow using the periodic perturbation has been attempted in various types of flows. Battacharjee et al. (1986) applied the acoustic perturbation to the shear layer over the backward-facing step and revealed that the promotion of reattachment was obtained by the enhancement of the spread of shear layer. Chun and Sung (1996) discovered that the reattachment promotion was caused by the enhancement of the entrainment in the shear layer due to the vortex merging.

Though these reports explain the enhancement of the mixing in terms of the vortex structure, its relation to the momentum transfer in the Reynolds averaged sense remains unexplained. Yoshioka et al. (1998) have made the PIV measurement in the same flow but with lower Reynolds number and reported the time averaged velocity as well as Reynolds stresses. They have postulated that the large scale vortical structure periodically induced by the perturbation play a major role in the enhancement of momentum transfer across the shear layer. Since they have reported only the time averaged data, the details of the effect of the induced vortices on the momentum transfer remained unclear.

The aim of the present study is to find the relation between the large scale vortex structure induced by the periodic perturbation and the momentum transfer on the basis of the mean momentum equation. To this end, the periodically fluctuating velocity field is investigated by applying the two-dimensional particle imaging velocimetry (PIV) together with the phase averaging technique synchronized with the given perturbation. The transport terms of the phase-averaged momentum equation are then estimated and compared with the periodic velocity field.

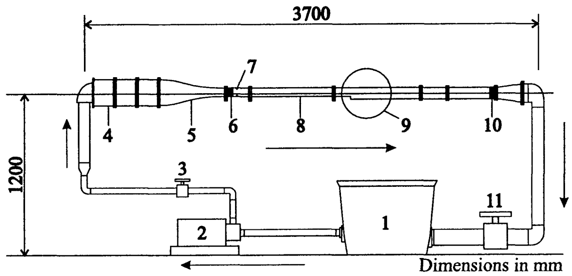

Fig. 1 Water channel facility

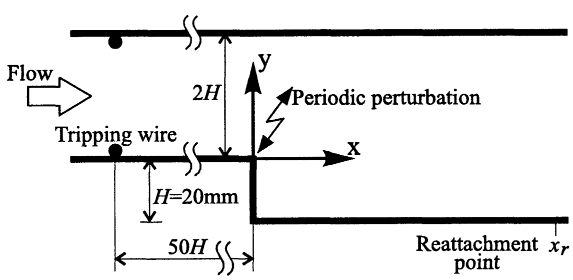

Fig. 2 Schematic of the test section

EXPERIMENTAL SETUP

The experiments were performed in a closed loop facility as shown in Fig. 1, using water at laboratory temperature. The flow was driven by a pump **2** (0.75kW) and passed through the settling chamber **4**, contract section **5** (contraction ratio is 0.12) and honeycomb **6**, before entering the test section **9**. At the upstream of the test section, the water passed through the rectangular channel of 40mm high and 240mm wide. In this channel, two tripping wires **7** were fitted on each sidewall to promote the transition. Another honeycomb **10** was set in the downstream of the test section to avoid the corner effect.

The test section, as shown in Fig. 2, was made of acrylic resin to enable the flow visualization. The backward-facing step was located in this section. The expansion ratio was 1.5, the step height $H =$ 20mm, the inlet channel width and span were $2H$ and $12H$, respectively. A spanwise slit, 1mm in width, was set up at the step edge, as shown in Fig. 3. The periodic perturbation was introduced through this slit as an alternating suction and injection in the direction 45 degrees relative to the streamwise direction. The perturbation velocity v_e was given by

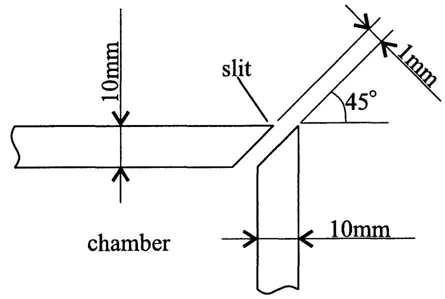

Fig. 3 Details of the step edge

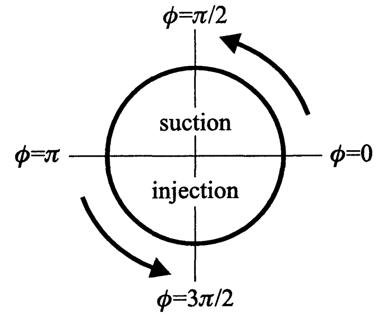

Fig. 4 Phase angle of the perturbation

$$v_e = V_e \sin(2\pi f_e t) = V_e \sin\phi, \qquad (1)$$

where V_e is the amplitude, f_e is the frequency and ϕ is the phase angle of the perturbation. It was generated by driving a piston by a stepping motor and introduced to the chamber inside of the step edge through a plastic tube. The stepping motor was driven by the control signal which followed the equation (1) generated by the personal computer. The relation between ϕ value and phase angle is shown in Fig. 4.

As illustrated in Fig. 2, the origin of Cartesian coordinates system was fixed at the center of the step edge. The x-axis was directed downstream and the y-axis was directed to the opposite side wall.

VELOCITY MEASUREMENT

PIV Technique

The velocity was measured by an in-house-made PIV system. The Nylon12 particles of 60μm in mean diameter and 1.02 in specific gravity were suspended in water as the tracer. The flow field was visualized by a Xenon stroboscopic light sheet and the motions of the tracers were taken by a monochromatic CCD camera.

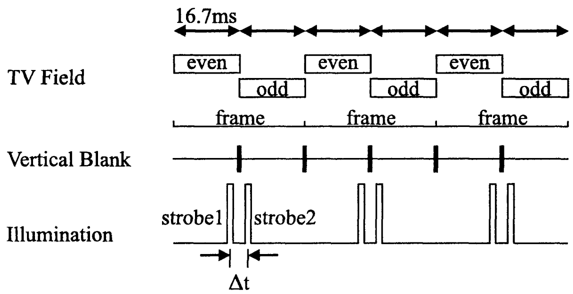

Fig. 5 Timing chart of the illumination for the PIV measurement

Figure 5 shows the timing of the illumination. In the present case, two independent stroboscopes (strobe1 and strobe2 showed in Fig. 5) were employed to keep enough input-power for the flushes. In each frame, the image exposed in the odd field was delayed 7.6 ms from the image exposed in the even field. The lamp-input power for the each flash was 1.7J/Flash with half-width duration around 18-23μs. The width of the light sheet at the test section was around 2mm.

The obtained images were directly digitized by a frame grabber (8bit, 640×480 pixels) equipped in a personal computer. The spatial resolution corresponding to one pixel was approximately 150μm. Images were grouped according to their perturbation phases and stored into a hard disk for further calculation that was conducted after the experiment. The number of the taken images was 1000 in every phase.

Each digitized frame image was separated to even and odd image before the velocity computation. The separated field images were vertically interpolated so that they have the same number of the horizontal lines as the TV frame. From the pair of the even and odd images, velocity vector distributions were computed by means of the cross-correlation method (Adrian, 1991).

Experimental Condition

In the present study, Re_H based on the center velocity at the inlet channel U_c and step height H was fixed to $Re_H = 3700$. The perturbation frequency was fixed to $St = 0.19$, where St was the non-dimensional frequency based on the perturbation frequency f_e, H and U_c. This frequency was almost close to the most effective frequency on the promotion of the reattachment (Chun and Sung, 1996). At this frequency, the reattachment length was reduced by around 30% in the present experiment. The velocity and Reynolds stress profiles show the inlet-flow is developed turbulent channel flow.

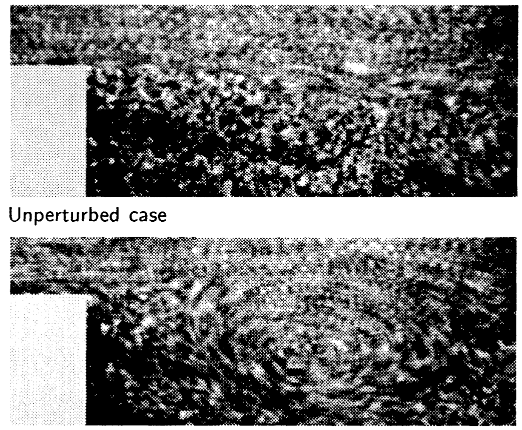

(a) Unperturbed case

(b) Perturbed case

Fig. 6 Flow visualization immediately behind the step edge

RESULTS AND DISCUSSION

Flow Visualization

Figure 6 shows the flow visualization immediately behind the step. The white rectangle at the left-bottom corner in each picture shows the step. In unperturbed case, a row of the relatively small vortices are observed in the separated shear layer, see Fig. 6(a). In perturbed case, a clockwise and a counter-clockwise vortex are shed alternately from the step edge in each perturbation cycle. At the injecting phase in the perturbed case as shown in Fig. 6(b), a large scale clockwise vortex, extending the order of the step height, is observed. This shed vortex flows towards downstream. At the maximum sucking phase (not shown), a relatively weak counter-clockwise vortex is shed.

Flow Structure in the Separated Shear Layer

The phase averaged velocity vectors in each perturbation phase are shown in Fig. 7. The filled rectangle at the left-bottom corner shows the step. The meandering of the ensemble-averaged streamlines are found in the separated shear layer indicating the effect of the periodic perturbation, though there are no indication of vortex roll-up just at the step edge. The first roll-up is found at $\phi = \pi$ (switching from suction to injection) denoted by '1' in Fig. 7(c). This clockwise vortex is convected and grows as seen in Fig. 7(d) and (a) (denoted by '2' and '3')

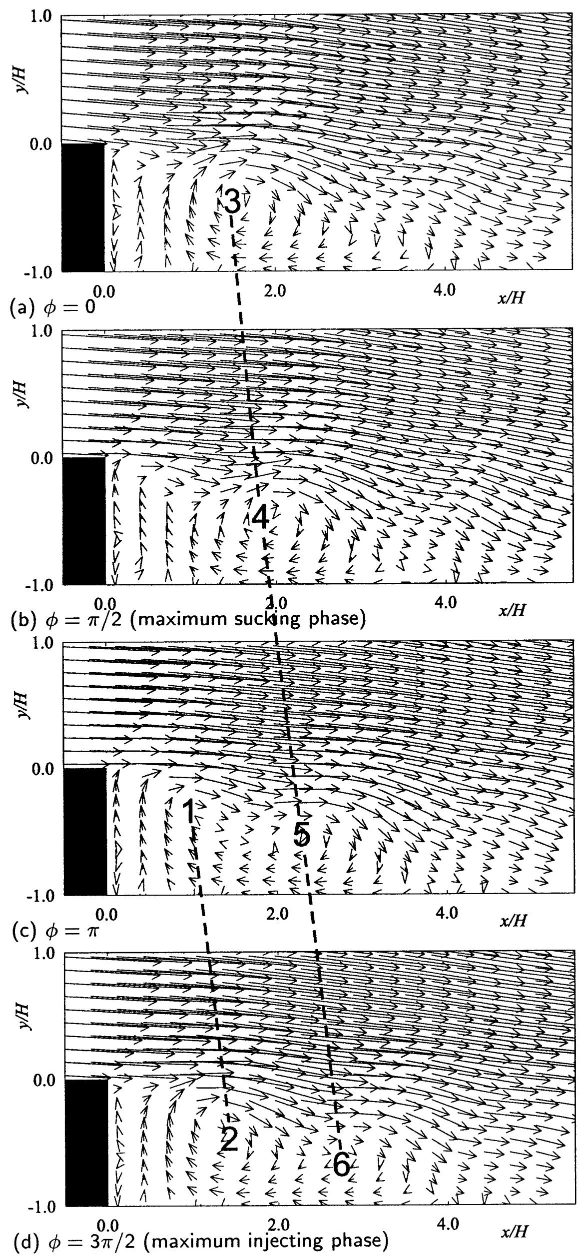

Fig. 7 Phase averaged velocity field

and reaches its maximum at $\phi = \pi/2$ (maximum sucking phase, denoted by '4') and then decays further. The shed vortex visualized in Fig. 6 corresponds to the vortex structure successively transported downstream shown in Figs. 7(a)-(d)

Figure 8 shows the phase averaged vorticity distribution. The filled triangle on the x axis of each figure denotes the time-averaged reattachment point.

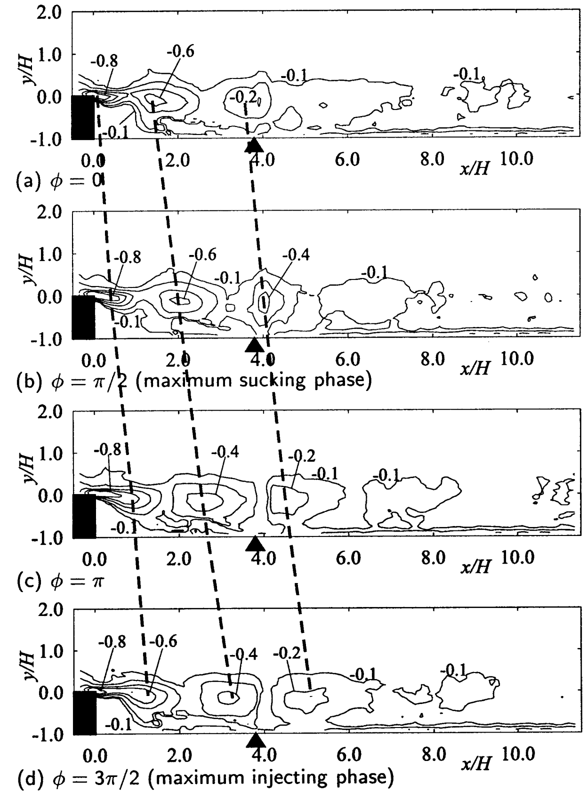

Fig. 8 Phase averaged vorticity distribution

The region of concentrated negative vorticity is initiated at the edge of the step when the injection reaches its maximum ($\phi = 3\pi/2$, Fig. 8(d)). This region is convected successively downstream with phase velocity approximately equal to 30% of U_c, denoted by dotted line in Fig. 8. The magnitude of the local maximum of vorticity monotonically decreases, while the area increases over three cycles in time and beyond the reattachment point in space.

To investigate the vortex motion in the separated shear layer introduced by the periodic perturbation, the pressure distribution is estimated here. The instantaneous velocity $\hat{u}$ and pressure $\hat{p}$ is decomposed to three levels:

$$\hat{u}_i = U_i + u_i = U_i + \tilde{u}_i + u_i' = \langle U_i \rangle + u_i' \quad (2)$$

$$\hat{p} = P + p = P + \tilde{p} + p' = \langle P \rangle + p' \quad (3)$$

where U and P are time averaged, $\langle U_i \rangle$ and $\langle P \rangle$ are phase averaged, $\tilde{u}_i$ and $\tilde{p}$ are periodic, u_i' and p' are turbulent component of the velocity and pressure, respectively. Periodic component means the fluctuation with frequency equal to that of the imposed perturbation. Phase averaged pressure distribution is calculated from the Poisson's equation of pressure:

$$\nabla^2\langle P\rangle = 2\rho\left(\frac{\partial\langle U\rangle}{\partial x}\frac{\partial\langle V\rangle}{\partial y} - \frac{\partial\langle U\rangle}{\partial y}\frac{\partial\langle V\rangle}{\partial x}\right). \quad (4)$$

Numerical integration is based on the SOR method, accomplished by substituting PIV velocity data into the right-hand side of equation (4) and assuming $\langle P\rangle = 0$ on the entire boundaries. Low pressure region is first observed immediately behind the edge of the step at the maximum sucking phase($\phi = \pi/2$, Fig. 9(b)). It moves downstream with increasing depth until it reaches to the minimum pressure at the beginning of the second cycle($\phi = 5\pi/2$, Fig. 9(b)), indicating the growth of vortex within this period of time. It should be noted here that the wall boundary condition assumed in the present investigation is physically unrealistic and the resulting pressure distribution especially near the wall needs further refinement. In spite of it, the information on the local pressure minimum is very helpful for understanding the vortical structure. The center of closed streamlines shown in Fig. 7, the local maximum of vorticity shown in Fig. 8 and the local minimum of pressure shown in Fig. 9 are coincident very well with each other, indicating that the periodic perturbation does induce the large scale periodic vortical structure.

The region of concentrated vorticity first appears at the maximum injecting phase. This vorticity perturbation is convected downstream and the shear layer begins to roll-up near the maximum sucking phase, generating the discrete vortex. It is convected downstream and grows to its maximum at the maximum sucking phase in the second cycle. Then it decays, though it continues to be recognized well within the third cycle, and beyond the reattachment point. The next question is how it is related to the momentum transfer in terms of the Reynolds averaged framework.

Effect of Momentum Transfer

The effect of large scale vortex motion introduced by the periodic perturbation on the momentum transfer across the separated shear layer is investigated. To discuss about the momentum transfer, after substituting equation (2) and (3) to the Navier-Stokes equation and taking phase average, the governing equation of this periodically perturbed flow field becomes:

$$\frac{\partial\langle U_iU_j\rangle}{\partial x_j} = -\frac{1}{\rho}\frac{\partial\langle P\rangle}{\partial x_i} + \frac{1}{\rho}\frac{\partial\langle \tau_{ij}\rangle}{\partial x_j} - \langle \mathcal{T}_i\rangle \quad (5)$$

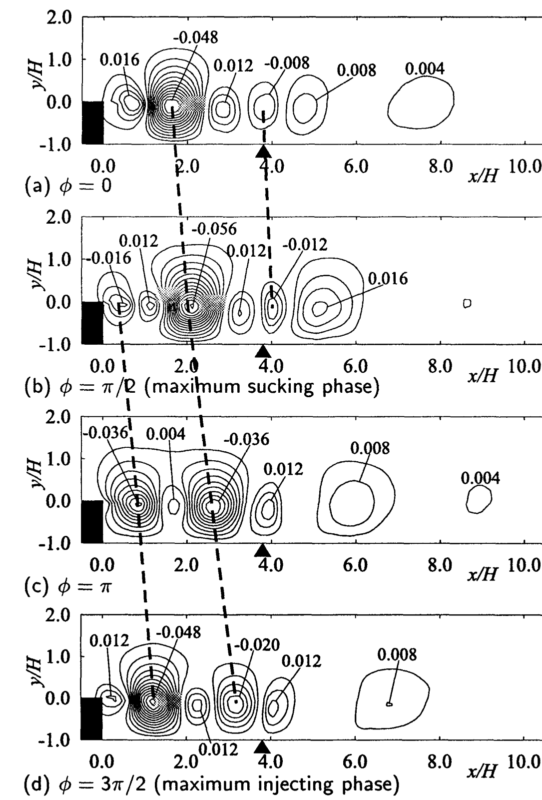

Fig. 9 Phase averaged pressure $\langle P\rangle/\rho U_c^2$ distribution

where,

$$\langle \mathcal{T}_i\rangle = \frac{\partial\langle u_iu_j\rangle}{\partial x_j} = \frac{\partial\langle u_i'u_j'\rangle}{\partial x_j} + \frac{\partial\langle \tilde{u}_i\tilde{u}_j\rangle}{\partial x_j}. \quad (6)$$

The term $\mathcal{T}_i$ stands for the momentum transfer due to the velocity fluctuation. $\mathcal{T}_U$ and $\mathcal{T}_V$ shown in Figs. 10 and 11 means the effect of the deceleration of U and V, respectively. Both $\mathcal{T}_U$ and $\mathcal{T}_V$ values are relatively large in each perturbation phase in the shear layer where the gradient of the their components, Reynolds stresses, are relatively large. Compared with the pressure distribution, the relation between the high-$\mathcal{T}_U$-value regions shown in Fig. 10 and the locations of vortices is not clear. On the other hand, $\mathcal{T}_V$ is relatively large where the vortices exist compared with the vortex structure shown in the velocity vectors (Fig. 7), vorticity distribution (Fig. 8) and pressure distribution (Fig. 9). This indicates that the vortices induced by the periodic perturbation enhances the deceleration of U and V, but V is more directly effected by the convecting vortex structure. This effect enhances the momentum transport across the separated shear layer.

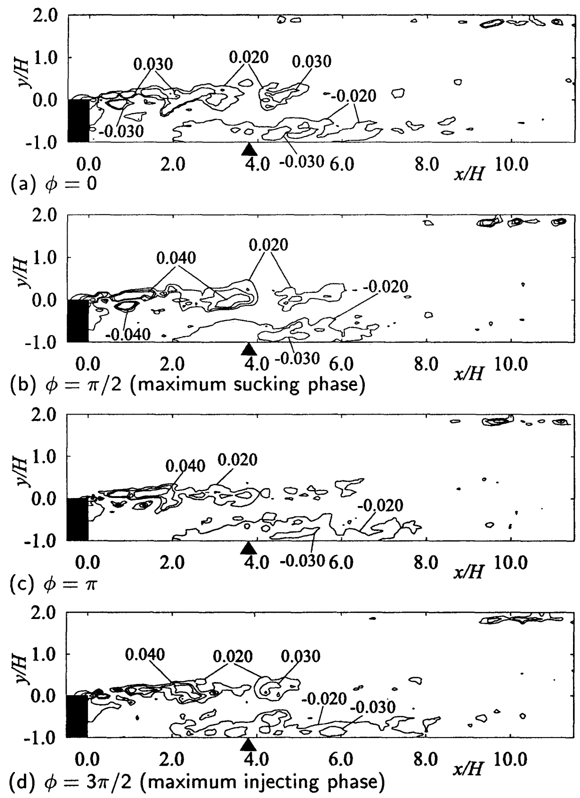

Fig. 10 Phase averaged $\langle \mathcal{T}_U \rangle / (U_c^2/H)$ distribution

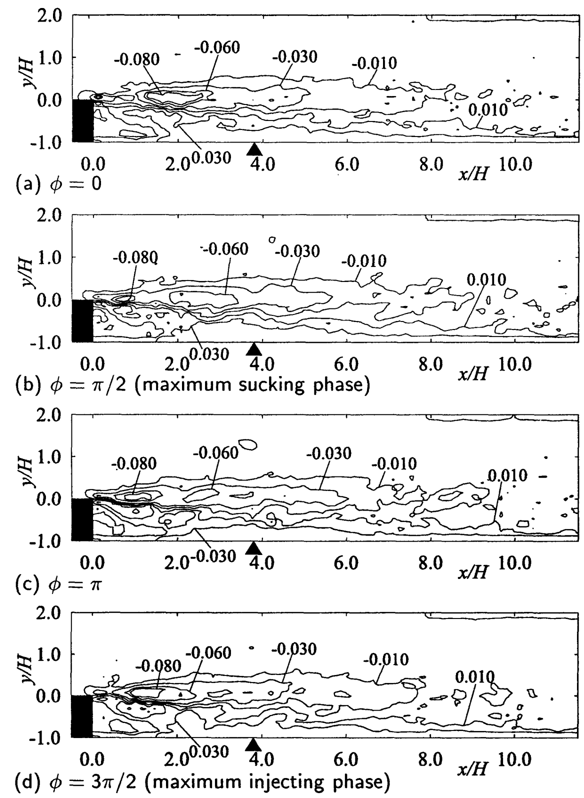

Fig. 11 Phase averaged $\langle \mathcal{T}_V \rangle / (U_c^2/H)$ distribution

CONCLUDING REMARKS

The effect of periodic perturbation on the turbulent separated flow over the backward-facing step is experimentally investigated in terms of the phase average synchronized with the perturbation.

Phase averaged velocity, vorticity and pressure distribution show that the vorticity perturbation is introduced at the maximum injecting phase and convected downstream. The shear layer begins to roll-up near the maximum sucking phase and a discrete vortex is generated. This vortex, being convected downstream, grows to its maximum at the maximum sucking phase in the second cycle.

According to the investigation on the phase averaged momentum transport in terms of the phase averaged Navier-Stokes equation, momentum transfer across the shear layer is enhanced by the introduced vortices.

ACKNOWLEDGEMENT

The financial support for the present work has been provided by Keio University. The authors are grateful to Prof. K. Nishino of Yokohama National University, Mr. M. Abe and Ms. A. Fujiwara of Keio University for their valuable advises on the PIV measurement and also to EBARA Research co., ltd. for facilitating the pump system.

REFERENCES

Adrian, R. J., 1991, "Particle-Imaging Technique for Experimental Fluid Mechanics," *Annual Review of Fluid Mechanics*, Vol. 23, pp. 261-394.

Bhattacharjee. S., Scheelke, B. and Troutt,T. R., 1986, "Modification of Vortex Interactions in a Reattaching Separated Flow," *AIAA Journal*, Vol. 24, pp. 623-629.

Chun, K. B. and Sung, H. J., 1996, "Control of Turbulent Separated Flow Over a Backward-facing Step by Local Forcing," *Experiments in Fluids*, Vol. 21, pp. 417-426.

Yoshioka, S., Obi, S. and Masuda, S., 1998, "Role of the Vortex Motion in the Periodically Perturbed Turbulent Flow over the Backward-facing Step," *Proc. Fourth KSME-JSME Fluids Engineering Conference*, pp. 585-588.